ON THE BEHAVIOUR OF THE HYSTERETIC WIRE-ROPE ISOLATORS UNDER RANDOM EXCITATION

IULIAN GIRIP[1], ŞTEFANIA DONESCU[2], MIHAELA POIENARIU[3], LIGIA MUNTEANU[1]

Abstract. Difficulties in characterizing of behavior of the wire-rope isolators under random excitation is the motivation for investigation of the modified Bouc-Wen model in the spirit of Baber and Noori, in order to include the experimentally observed stiffness and strength degradation, and pinching, respectively. The prediction of the behavior of such structures with hysteretic shear behavior under random excitation is investigated in this paper. The model is verified for the case of harmonic excitation with a range of exciting frequencies and amplitude levels, on the base of reported data in literature.

Key words: Wire-rope isolator, Bouc-Wen model, stiffness and strength degradation, pinching.

1. INTRODUCTION

The wire-rope isolators are assemblies made of stranded wire ropes which are wrapped around a metallic or fibrous core (Fig.1a). The section of a rope is shown in Fig.1b. The rope is wound in the form of helix and held between metal retainers (Fig.1c) [1–2]. The diameter of the wire rope, the number of strands, the rope length, the cable twist or lay, the number of ropes per twist section and the fashion of metal retainer are the main parameters that characterize the assembly. The rubbing and sliding friction between the strands of wire rope define the damping and the deformation of isolators.

For steady periodic excitation, the wire-rope isolators exhibit nonlinear hysteretic behavior due to the fact that the hysteretic loops depend on the vibration level, being almost independent of frequency [3–6]. Information from damage of the wire-rope isolators surveyed after realistic cyclic and arbitrary dynamic loadings and the experimentally observed characteristics, indicate that such

[1] Institute of Solid Mechanics, Romanian Academy, Bucharest
[2] Technical University of Civil Engineering, Bucharest
[3] "Spiru Haret" University, Bucharest

Rom. J. Techn. Sci. – Appl. Mechanics, Vol. 58, N° 3, P. 209–221, Bucharest, 2013

structures exhibit a wide variety of hysteretic features including inelastic load-displacement law without distinct yield point, progressive loss of lateral stiffness in each loading cycle (stiffness degradation), degradation of strength when cyclically load is done to the same displacement level (strength degradation) and pinching [7, 8]. The pinching behavior is due to slipping during force reversal.

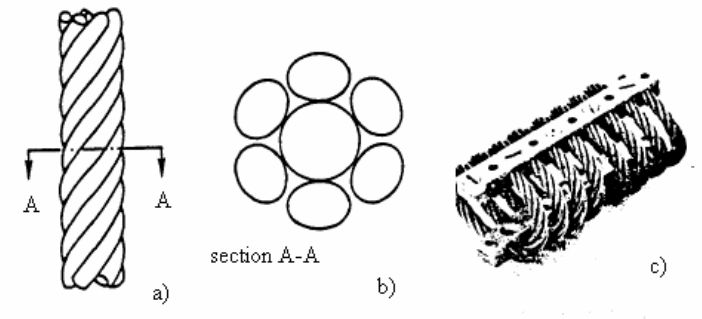

Fig.1 – a) Thw wire-rope geometry; b) section A-A of the rope; c) helical shape of isolators.

The smoothly varying Bow-Wen model is widely used for different loadings of hysteretic systems [9–16]. The model can be used also for including the pinching and degradation features [11, 17].

This paper tries to predict the behavior of the wire-rope isolators with hysteretic shear behavior under random excitations such earthquakes. The idea is to augment the Bouc-Wen model in the spirit of Baber and Noor [18], in order to include the experimentally observed characteristics such as the stiffness and strength degradation and pinching, respectively. The model is verified for the case of harmonic excitation with a range of exciting frequencies and amplitude levels, on the base of reported data in literature [5, 16].

2. MODEL DESCRIPTION

The helical wire-rope devices are used as vibration isolation systems. Fig.2 shows the model of the wire-rope isolator arranged as a hanging shaking platform [5]. Two rigid plates are hung in parallel on a trestle, through frictionless hinges connected with four rigid steel tubes to form a double pendulum system. Additional guiding rollers prevent lateral motion of the system. The isolator is mounted and fixed with its aluminum retainer bars to the upper and lower plates for hysteretic shear behavior tests. The upper plate of the mass m on the top of the isolator is fixed horizontally to the trestle through a force transducer. The lower plate of mass m under the isolator is excited on one end and connected to the displacement transducer on the others. The lower mass is acted by the forcing

force $F(t)$. The relative displacement between plates is $u = x_2 - x_1$. The motion equation written with respect to u is

$$m\ddot{u} + c\dot{u} + R(u,z,t) = F(t), \tag{1}$$

where $c\dot{u}$ is damping restoring force, with c the damping coefficient, and $R(u,z,t)$ is the non-damping restoring force

$$R(u,z,t) = \alpha k u + (1-\alpha)kz, \tag{2}$$

composed by the linear restoring force αkz, and the hysteretic restoring force $(1-\alpha)kz$, where $0 < \alpha < 1$ is the rigidity ratio representing the relative participations of the linear and nonlinear terms. Here, $z(t)$ is the hysteretic auxiliary variable representing the hysteretic displacement function of the time history of u. It is related to $u(t)$ through the constitutive law the force-displacement [17]

$$\eta \frac{\mathrm{d}z}{\mathrm{d}u} = h(z)\left(A - \nu(\beta \operatorname{sgn}(\dot{u}) |z|^{n-1} z + \gamma |z|^n)\right), \tag{3}$$

where $h(z)$ is the pinching function (for $h = 1$ the function is not pinch), A a parameter that controls the tangent stiffness and ultimate hysteretic strength, β, γ, n are the hysteretic shape parameters and ν, η the strength and stiffness degradation functions (for $\nu = \eta = 1$ the model is not degrading). These functions depend on the dissipated hysteretic energy. The law (3) extends the Bouc-Wen model by including the pinching function.

By setting $\mathrm{d}z/\mathrm{d}u$ to zero in (3) and solving it for z, we obtain the ultimate hysteretic strength z_u

$$z_u = \left(\frac{A}{\nu(\beta+\gamma)}\right)^{1/n}. \tag{4}$$

The pinching function $h(z)$ is taken under the form [15]

$$h(z) = 1 - \zeta_1 \exp(-(z \operatorname{sgn}(\dot{u}) - z_u)^2 / \zeta_2^2), \tag{5}$$

where $\zeta_1 < 1$ is a variable which controls the magnitude of initial drop in the slope $\mathrm{d}z/\mathrm{d}u$, and ζ_2 a variable which controls the rate of change of the slope $\mathrm{d}z/\mathrm{d}u$.

By dividing the equation (1) by m, we obtain

$$\ddot{u} + 2\zeta_0 \omega_0 \dot{u} + \alpha \omega_0^2 u + (1-\alpha)\omega_0^2 z = f(t), \tag{6}$$

where $f(t)$ is the mass-normalized forcing function, $\omega_0 = \sqrt{k_i / m}$, with k_i, the initial stiffness, $\zeta_0 = c / 2\sqrt{k_i m}$ – the linear stiffness.

The identification procedure is based on the signification of each unknown parameter $\{\alpha, A, \beta, \gamma, n, \zeta_1, \zeta_2\}$ and two unknown functions $\{\nu, \eta\}$. We are interested to identify what parameters and functions of interest can be evaluated directly from the features of the experimental data.

In the following we will see that α, β, γ and n can be directly evaluated from the experiment, i.e. the restoring force against displacement.

The system properties are evaluated from the model. The first natural frequency is calculated as $\sqrt{k_i / m}$, where m is the estimated mass of the system and k_i the initial stiffness.

The value of the linear damping ratio ξ_0 may be chosen within the range 0.01 and 0.05 [17].

The problem of the redundant parameters in (3) was discussed in [19]. It was proved that A is redundant and, as a consequence, it is assumed to be 1. The parameter α is calculated as the ration of the final tangent stiffness k_f to initial stiffness k_i

$$\alpha = \frac{k_f}{k_i}, \tag{7}$$

$$k_i = \frac{\mathrm{d}R}{\mathrm{d}u}\Big|_{z=u=0} = k\ , \quad k_f = \frac{\mathrm{d}R}{\mathrm{d}u}\Big|_{z=z_u} = \alpha k\ . \tag{8}$$

The equations for loading paths are obtained from (3) for $\nu = \eta = 1$ and $h = 1$

$$\frac{\mathrm{d}z}{\mathrm{d}u} = 1 - (\beta + \gamma) z^n\ ,\ z\dot{u} > 0\ , \tag{9}$$

and for unloading case

$$\frac{\mathrm{d}z}{\mathrm{d}u} = 1 - (\gamma - \beta) z^n\ ,\ z\dot{u} < 0\ . \tag{10}$$

The parameters β and γ are determined from (3) for $h = 1$ and $\nu = \eta = 1$ written as

$$\frac{\mathrm{d}z}{\mathrm{d}u} = 1 - (\beta + \gamma) z^n\ ,\ z \geq 0\ ,\ \dot{u} \geq 0\ , \tag{11}$$

$$\frac{\mathrm{d}z}{\mathrm{d}u} = 1-(\gamma-\beta)z^n,\ z \geq 0,\ \dot{u} < 0, \tag{12}$$

$$\frac{\mathrm{d}z}{\mathrm{d}u} = 1+(-1)^{n+1}(\beta+\gamma)z^n,\ z < 0,\ \dot{u} < 0, \tag{13}$$

$$\frac{\mathrm{d}z}{\mathrm{d}u} = 1+(-1)^{n+1}(\gamma-\beta)z^n,\ z \leq 0,\ \dot{u} \geq 0. \tag{14}$$

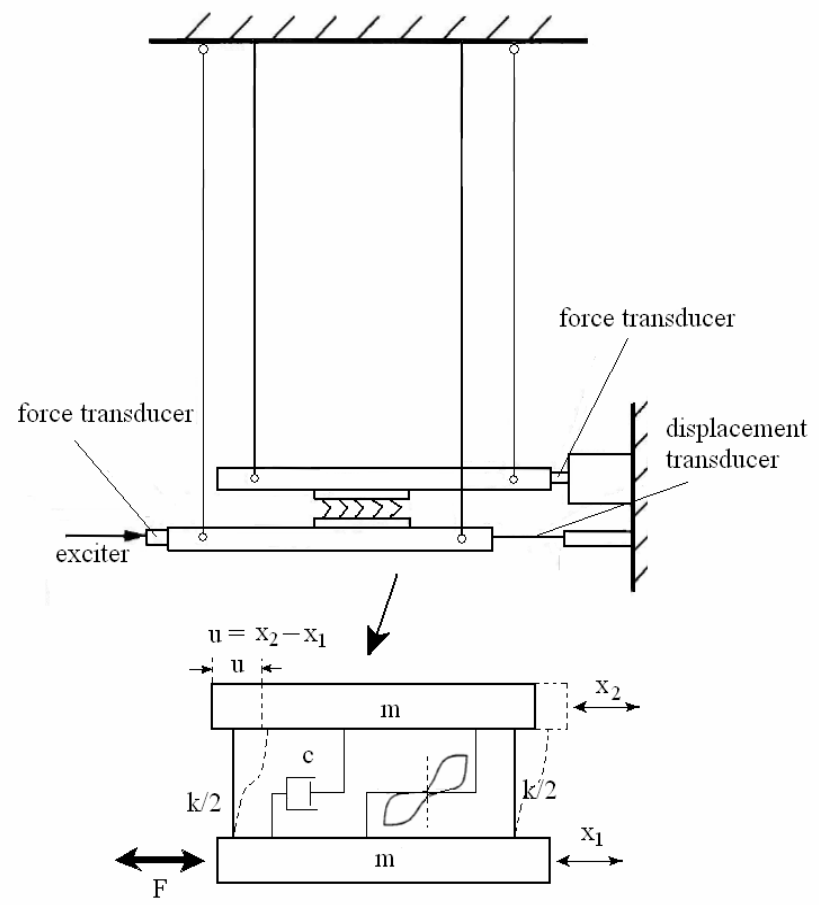

Fig. 2 – The model of the wire-rope isolator arranged as a hanging shaking platform [5].

In what concerns the parameter n, we obtain from (4) and (9) for non-degrading case $\nu = 1$

$$\frac{\mathrm{d}z}{\mathrm{d}u} = 1 - \left(\frac{z}{z_u} \right)^n . \tag{15}$$

The shape parameters are chosen so that $\beta + \gamma > 0$ and $\gamma - \beta \le 0$, with $\beta > 0$ in order to have a positive energy dissipation.

In what concerns the stiffness and strength degradation functions ν and η, they are related to the dissipated hysteretic energy W [17]

$$\nu(W) = 1 + \delta_\nu W , \quad \eta(W) = 1 + \delta_\eta W , \tag{16}$$

where

$$W = \omega_0^2 \left(1 - \frac{k_f}{k_i} \right) \int_{t_0}^{t_f} z\dot{u} \, \mathrm{d}t , \quad 0 < \frac{k_f}{k_i} < 1 . \tag{17}$$

The energy W is the cumulative dissipated hysteretic energy, in other words the sum of the loops areas. The functions $\nu(W)$ and $\eta(W)$ control the strength and stiffness degradations. The $\delta_\nu > 0$ and $\delta_\eta > 0$, are unknown parameters. The stiffness degradation occurs when the elastic stiffness degrades with increasing ductility, as shown in Fig. 3 to left. This behavior occurs due to geometric effects. The strength degradation is described by reducing the capacity in the backbone curve, as shown in Fig. 3 to right. Fig. 4 shows the pinching behavior in the diagram $\mathrm{d}z/\mathrm{d}u$ against z/z_u, where z_u is the ultimate hysteretic strength given by (4). The pinching is the typical behavior of structures that buckle when subjected to compressive loads. This behavior usually is the result of cracks or slips.

To identify the remaining parameters $\delta_\nu, \delta_\eta, \zeta_1$ and ζ_2, that cannot be directly evaluated from the experiment, a genetic algorithm can be applied in the same manners as in [11], by using experimental data.

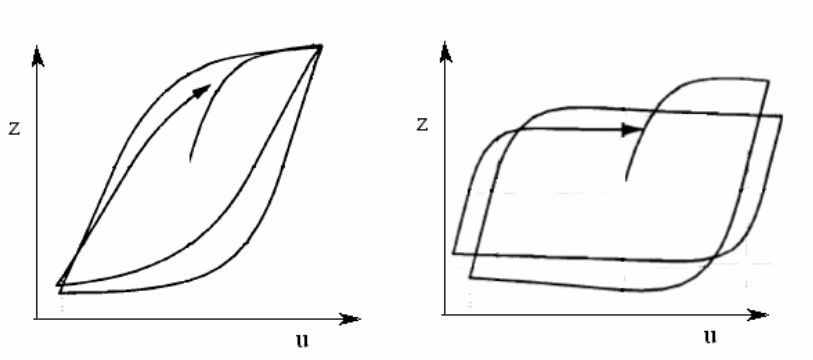

Fig. 3 – Stiffness degradation behavior (left); strength degradation behavior (right) [17].

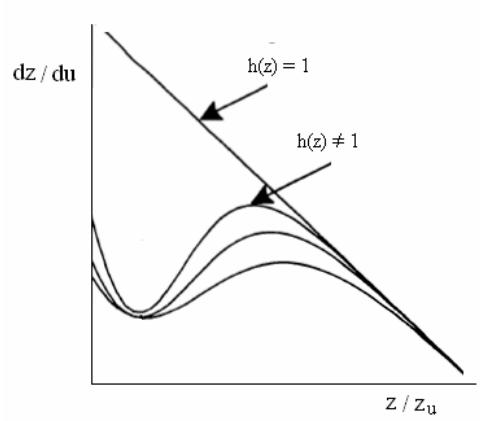

Fig. 4 – Pinching behavior for $h(z) \neq 1$ [17].

4. RESULTS

The model is verified firstly for the case of harmonic excitation. The numerical simulation was conducted using experimental data reported in [3] and [11]. The excitation signal is supplied by sine harmonic excitation. The restoring hysteretic force, acceleration and displacements signals are measured for a number of 11 frequencies ranging from 5Hz to 50Hz, with at least 5 different amplitudes levels in each case, recorded in a synchronous manner on a tape recorder and observed with a digital signal analyzer. Figure 5 shows the experimental loop of the hysteretic restoring force against the displacement, for the case of steady periodic excitation without filtering [5]. After filtering, the loop is shown in Fig. 6. The necessity of filtering is due to the non-synchronism which may appear between the restoring force and displacement during recording. This non-synchronism can distort the shape and area of the loop. Therefore, these signals must be simultaneously measured at each recording time.

The parameters α, β, γ and n are evaluated directly from the experiment (Fig. 6), while the parameters $\delta_\nu, \delta_\eta, \zeta_1$ and ζ_2 are obtained from an identification procedure based on the genetic algorithm.

The parameters are summarized in Table 1.

Table 1
The parameter values used in the numerical simulation for the case of harmonic excitation

α	β	γ	n	ζ_1	ζ_2	δ_ν	δ_η
0.26	0.33	0.88	1.89	0.42	0.33	0.11	0.10

The results for harmonic excitation agree very well with the results presented in [5]. The obtained hysteretic loops show typical nonlinearity (for example Fig. 7 shows the restoring force against the displacement for 6 Hz).

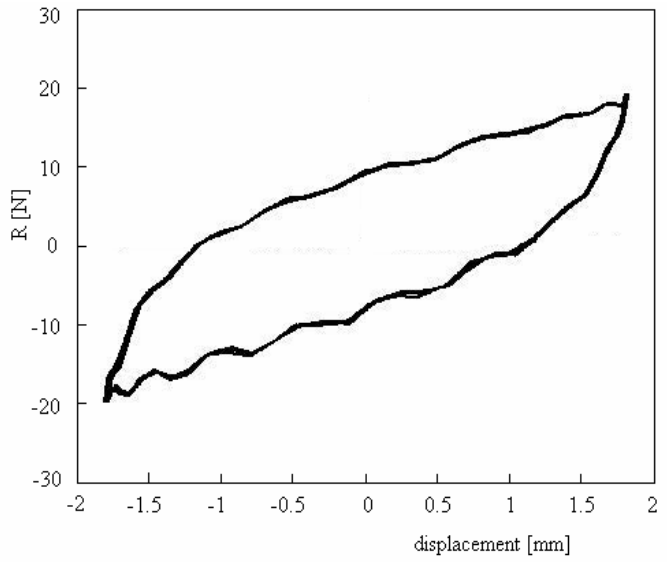

Fig. 5 – Experimental hysteretic loop of restoring force against displacement without filtering [5].

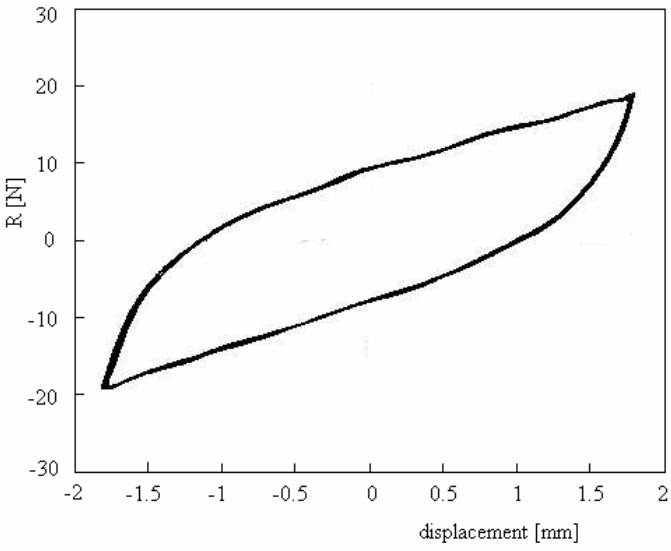

Fig. 6 – Experimental hysteretic loop of restoring force against displacement loop with filtering [5].

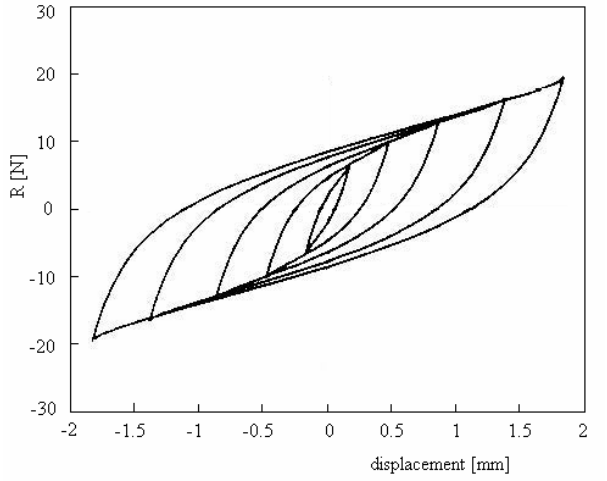

Fig. 7 – Restoring force against displacement at 6 Hz.

Next, the case of the random excitation is analyzed. The excitation signal is represented as the sum of a number of sinusoids of random phase and frequency $0.25l + \pi/100$, $l = 20,...,40$ [20]. The frequency range is approximately 5–10Hz. The amplitude of the excitation is chosen so that the strong nonlinearities and sliding of the isolator to be manifested. As written by other researchers [13], the genetic algorithm gives best results with a few cycles of the non-linear response. The first results are presented in Figs. 8 and 9.

The numerical simulation of the hysteretic loop of the excitation against the displacement is shown in Fig. 8. Although this diagram looks like to experimental hysteretic loop without filtering shown in Fig. 5, it has nothing to do with the synchronism between the excitation force and displacement. Its character is done by the random feature of the loading. A similar behavior was obtained in [21] for friction pendulum systems under severe dynamic loading such as earthquakes.

The parameters are summarized in Table 2.

Table 2

The parameter values used in the numerical simulation in the case of random excitation

α	β	γ	n	ζ_1	ζ_2	δ_ν	δ_η
0.47	0.87	0,90	2.15	0.94	0.72	0.21	0.22

Effects of degradation parameters upon the time variation of u is shown in Fig. 10 at 5 Hz. The numerical simulation of the evolution of the hysteretic displacement function $z(t)$ with respect to the relative displacement between plates, u is shown in Fig. 11, for 5Hz. Reducing the capacity in the backbone of the

hysteretic curve and the increasing ductility in material leads to large displacement in both situations.

The effect of pinching in the hysteretic loop of the restoring force against displacement 5 Hz is presented in Fig.11. The double-valued of the restoring force for all times except when passes through the origin leads to pinching of the curve in origin.

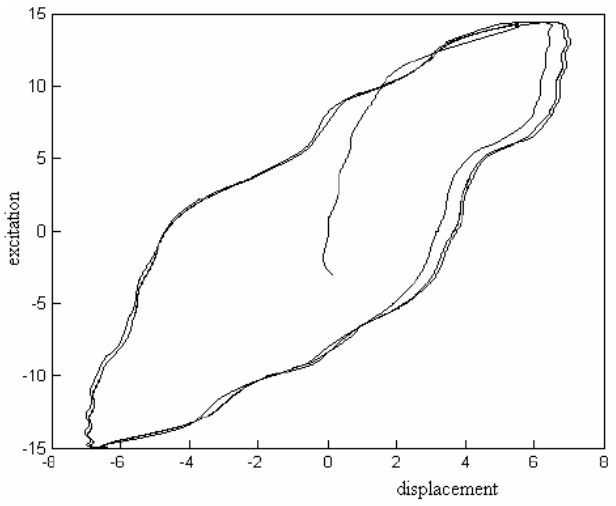

Fig. 8 – Theoretical hysteretic loop of the excitation against the displacement.

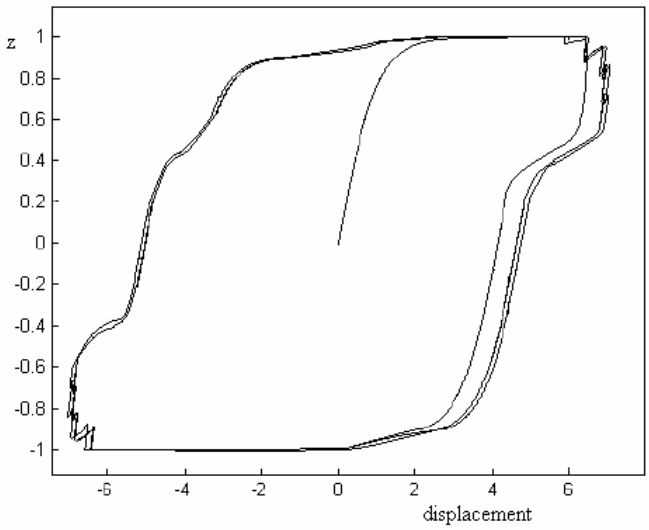

Fig. 9 – Theoretical hysteretic loop $z(t)$ against the relative displacement u .

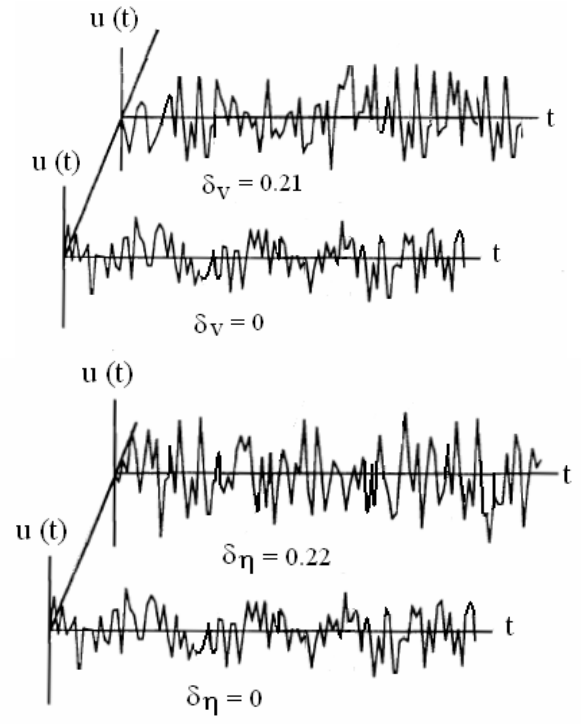

Fig. 10 – Effect of the stiffness degradation δ_v parameter on u at 5 Hz (left); effect of the strength degradation parameter δ_η on u at 5 Hz (right).

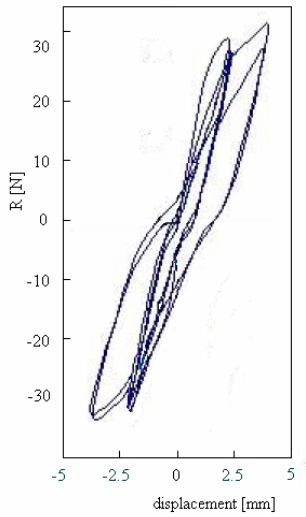

Fig. 11 – Effect of pinching in origin of the hysteretic loop of restoring force against displacement at 5 Hz.

5. CONCLUSIONS

This paper tries to predict the behavior of the wire-rope isolators with hysteretic shear behavior under random excitation. The Bouc-Wen model is modified in the spirit of Baber and Noori in order to include the experimentally observed characteristics such as the stiffness and strength degradation and pinching, respectively. The model is verified for the case of harmonic excitation with a range of exciting frequencies and amplitude levels, on the base of reported data in literature. For random excitation, the wire-rope isolator was subjected to large deformations. It was observed that the isolator exhibits reducing of its capacity in the backbone of the hysteretic loop and the increasing ductility, respectively, as effects on the degradation. The hysteretic loop of restoring force against displacement is pinched at the origin for the random excitation.

Acknowledgements. This research was elaborated through the PN-II-PT-PCCA-2011-3.1-0190 Project of the National Authority for Scientific Research (ANCS, UEFISCSU), Romania. The authors acknowledge the similar and equal contributions to this article.

REFERENCES

1. GILBERT, C., LEKUCH, H., *Severe service requires strenuous shock/ vibration testing*, Military Electronics/ Countermeasures, ICMD of North America Corp., **8**, *11*, pp. 34–41, 1982.
2. TINKER, M.L., *Modeling of nonlinear vibration isolatoirs using advanced continuous simulation language (ACSL),* Report 1–10, 2000.
3. WONG, C.W., NI, Y.Q., LAU, S.L., *Steady-State Oscillation of Hysteretic Differential Model I: Response Analysis*, J. Eng. Mech., ASCE, **120**, 1994.
4. WONG, C.W., NI, Y.Q., KO, J.M., *Steady-State Oscillation of Hysteretic Differential Model II: Performance Analysis*, J. Eng. Mech., ASCE, **120**, 1994.
5. KO, J.M., NI, Y.Q., TIAN, Q.L., *Hysteretic Behavior and Empirical Modeling of a Wire-Cable Vibration Isolator*, Int. J Anal. Exp. Modal Anal., **7**, *2*, pp. 111–127, 1992.
6. Ni, Y.Q., Ko, J.M., Wong, C.W., *Identification of non-linear hysteretic isolators from periodic vibration tests*, Journal of Sound and Vibration, **217**, *4*, pp. 737–756, 1998.
7. DEMETRIADES, G.F., CONSTANTINOU, M.C., REINHORN, A.M., *Study of wire rope systems for seismic protection of equipment in buildings.* Engineering structures, **15**, pp. 321–334, 1993.
8. FUJITA, T., SASAKI, Y., FUJIMOTO, S., TSURUYA, C., *Seismic isolation of industrial facilities using lead-rubber bearings*. JSME International Journal: **111,** *3*, pp. 427–434, 1990.
9. BOUC, R., *Forced Vibration of Mechanical System With Hysteresis*, Proc. of 4th Conference on Nonlinear Oscillation, Prague, 1967.
10. WEN, Y.K., *Method for Random Vibration of Hysteretic Systems*, J .Fng. Mech. Div., ASCE, **102**, 1976.
11. SIRETEANU, T., GIUCLEA, M., MITU, A.M., *Identification of an extended Bouc-Wen model with application to seismic protection through hysteretic devices*, Computational Mechanics, **45**, *5*, pp. 431–441, 2010.
12. GIRIP, I., ŞTIUCA, P., MUNTEANU, L., *On a shape identification problem,* Rev. Roum. Sci. Techn., Méca. Appliquée, **55**, *3*, pp. 211–218, 2010.
13. POIENARIU, M., IONESCU, M.F., GIRIP, I., MUNTEANU, L., CHIROIU, V., *On the damped beams with hysteresis*, World Journal of Mechanics (WJM), Scientific Research Publishing, Inc. USA, **1**, *1*, pp. 6–14, 2011.

14. MUNTEANU, L., MOŞNEGUŢU, V., GIRIP, I., POPESCU, M.A., *On the influence of density on the wave propagation in fluids,* Rev. Roum. Sci. Techn. – Méc. Appl., **57**, *1*, pp. 63–70, 2012.
15. GIRIP, I., MUNTEANU, L. GLIOZZI, A., ch.5: *Inverse problems in the hysteresis modeling,* Inverse Problems and Computational Mechanics, Vol.1, Editura Academiei (eds. L.Marin, L.Munteanu, V.Chiroiu), 2011, pp. 125–146.
16. WONG, C.W., KOAND, J.M., NI, Y.Q., *Modeling the hysteresis curves of wire-cable isolators,* Report Dept. of Civil and Structural Engineering Hong Kong Polytechnic, Kowloon, 1994, pp. 644–648.
17. FOLIENTE, G.C., *Stochastic dynamic response of wood structural systems*, PhD Thesis, Virginia Polytechnic Institute and State University, Blacksburg, 1993.
18. BABER, T.T., NOORI, M.N., *Modelling General Hysteresis Behaviour and Random Vibration Application,* Journal of Vibration, Acoustics, Stress, and Reliability in Design. Transactions of the ASME, **108**, pp. 411–420, 1986.
19. MA, F., ZHANG, H., BOCKSTEDTE, A., FOLIENTE, G.C., PAEVERE, P., *Parameter Analysis of the Differential Model of Hysterezis*, J. of Appl. Mech. ASME, **71**, pp. 342–349, 2004.
20. STAMMERS, C.W., SIRETEANU, T., *Control of building seismic response by means of three semi-active friction dampers*, Journal of Sound and Vibration, **273,** *5*, pp. 745–759, 2000.
21. PANOS C. DIMIZAS AND VLASIS K. KOUMOUSIS, *System identification of non-linear hysteretic systems with application toi friction pendulum isolation systems*, 5th GRACM International Congress on Computational Mechanics GRACM 05 , Limassol, 29 June – 1 July, 2005, pp. 1–8.